Journal of Pharmacokinetics and Biopharmaceutics, Vol. 22, No. 6, 1994

The Relationship Between Receptor–Effector Unit Heterogeneity and the Shape of the Concentration–Effect Profile: Pharmacodynamic Implications

Amnon Hoffman[1,3] and Assaf Goldberg[2]

Received January 24, 1994—Final January 17, 1995

The apparent concentration–effect relationship is the ensemble of many effector units (such as individual cells or channels) that do not always exhibit a uniform stimulus–effect relationship. This concept is substantiated by many observations of heterogeneity in receptor–effector populations including hormone secreting cells, response to hormonal stimuli, activity pattern of second messengers, stimulus-evoked synaptic currents, and single ion channels. The relationship between drug concentration and magnitude of pharmacologic response is commonly described by the sigmoidal E_{max} model which was derived from the Hill equation. The sigmoidicity factor (N) in this model is assumed to be a pure mathematical parameter without physiological connotations. This work demonstrates that the numerical value of N (measured empirically) is the product of two factors: (i) the degree of heterogeneity of the effector subunits, i.e., the elemental component that upon drug stimulus contributes its pharmacological effect independently and does not interact with other subunits (it could range from a single receptor up to a whole tissue), and (ii) value of N^*—the shape factor of the subunits' concentration–effect relationship. A special case of this approach occurs when $N^* > 5$, which is an on–off case. Here N is determined by the distribution (density equation) of the subunit values. In case of heterogeneity of the microparameters of the effector subunits the apparent N will always have a lower value than N^*. According to this theory it can be concluded that without knowledge of the distribution of the microparameters no mechanistic interpretation can be deduced from the apparent N value. If in the future N^* can be determined by theoretical or experimental methods, the distribution function relating N^* to N can be calculated. The relevance of this theory is increased in view of the progress being made in advanced research techniques which may enable us to determine the concentration–effect relationship at the level of the individual effector unit.

KEY WORDS: concentration–effect; heterogeneity; pharmacodynamics; receptor; E_{max} model; dose response; shape factor; effector unit; Hill coefficient; sigmoidal E_{max} model.

INTRODUCTION

Most of the current conceptualization relating stimulus and effect regards the subeffector units (e.g., each unit that secretes neurotransmitters

[1]Department of Pharmacy, School of Pharmacy, The Hebrew University of Jerusalem, P.O. Box 12065 Jerusalem, Israel 91120.
[2]Department of Mathematics, The Hebrew University of Jerusalem, Jerusalem, Israel 91120.
[3]To whom correspondence should be addressed.

0090-466X/94/1200-0449$07.00/0

or hormones, contractile proteins in muscle cell, single ion channels) as a homogeneous population. This concept is questionable since it overlooks natural variability among subeffector units (e.g., diversity in a cell's age, stage of differentiation, or structure of receptor subtypes). Further, biological responses are often quantal in nature with characteristic amplitude distribution; research is revealing that heterogeneity of subeffector units is the rule in many biological systems (see Discussion). Subeffector heterogeneity provides a new perception of the apparent relationship between stimulus and effect; this paper highlights the pharmacodynamic implications of this phenomenon.

The concept that drug activity occurs by its interaction with a receptor substance has been a basic pharmacologic principle for over a century. This concept suggests that the drug interacts reversibly with a receptor and the resultant effect is proportional to the number of receptors occupied. This relationship can be described as:

$$\text{Drug } (D) + \text{Receptor } (R) \rightleftharpoons (DR) \rightarrow \text{Effect} \tag{1}$$

Rearrangement of this relationship produces Eq. (2) analogous to the Michaelis-Menten equation which correlates the effect (E) to free drug concentration (D), a dissociation constant for drug-receptor binding (Kd), and maximal effect (E_{max}) attainable when all the receptors (R_{tot}) are occupied by drug. This relationship is based on the assumption that

$$E = \frac{R^*}{R_{tot}}$$

where R^* represents activated or occupied receptors

$$R^* = \frac{R_{tot} D}{Kd + D} \quad \text{or} \quad E = \frac{E_{max} D}{Kd + D} \tag{2}$$

The theory and application of this relatively simple equation forms the basis for the understanding and use of kinetic–dynamic relationships. Ariens *et al.* (1) was the first to recognize and formulate the analogy between receptor systems and enzymes, an analogy based on the theory of "receptor" occupancy. In both systems the binding of the ligand precedes the "biochemical" reaction. In Eq. (2) the binding constant Kd, was replaced by EC_{50}, the drug concentration producing 50% of the maximal response, resulting in Eq. (3) the E_{max} model.

$$Effect = \frac{E_{max} C}{EC_{50} + C} \tag{3}$$

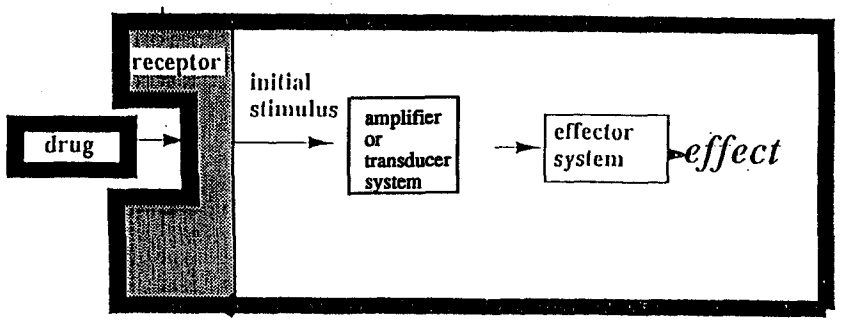

Fig. 1. Schematic illustration of the typical steps from drug binding to the receptor (the input signal) up to the pharmacologic effect (the output signal).

Interpretation of an EC_{50} value in terms of *Kd* (determined in receptor binding studies), in most cases flawed, e.g., transducer systems linking drug concentration to effect and the existence of "spare receptors." As shown in Fig. 1, the step of receptor occupancy should be followed by a successful coupling between the receptor and the effector system resulting in the induction of an intitial stimulus. This stimulus triggers a cascade or transduction of intracellular biochemical events that eventually lead to the final physiological or pharmacological response in the target cell.

A more flexible model for correlating drug concentration and effect is provided by the sigmoidal E_{max} model [Eq. (4)]. It brings in the additional concept of slope or steepness of the E_{max} curve by using the Hill coefficient (N) (3).

$$Effect = E_0 + \frac{E_{max} C^N}{EC_{50}^N + C^N} \tag{4}$$

In the theories linking drug binding and response at isolated tissues, the Hill coefficient was used to measure the cooperativity of the sytem (5,6). In general $N > 1$ is interpreted as the binding of one agonist molecule facilitating the binding of subsequent molecules.

The major difference between the signoidal E_{max} model and the E_{max} model is that in the sigmoidal model the parameter N provides an additional variable which can influence the gradient of the effect–concentration curve around EC_{50}.

Utilization of the sigmoidal E_{max} model to relate drug concentration and pharmacological response in intact animal and man was first proposed by Wagner (7). As indicated by Wagner and since then by many more researchers, the value of N in most cases is larger than 1 (the implicit N value in the simple E_{max} model). This fact actually stresses the clear advantage in

the empirical analysis of data using the sigmoidal E_{max} model. It is known that N which is often called the "shape factor," or "sigmoidicity factor" (7) need not be an integer. When N is greater than 1, the slope becomes sigmoidal and very steep and rapid changes in drug activity occur with small changes in drug concentrations. As N increases it becomes more difficult to carefully titrate a desired effect. Values of N greater than 5 approximate a response which behaves as an all-or-none phenomenon. It appears as if there is a threshold concentration below which no drug effect is seen but almost full response observed at concentrations just over the threshold. On the other hand, when N is less than 1, a shallow hyperbolic concentration–effect relationship is displayed, with changes in effects occurring over a wide range of drug concentrations.

The apparent pharmacological response is the sum of the effect of the drug on many subeffector units. Most of the "Receptor" theories linking drug binding and response assume that all the receptors involved with a defined activity are homogeneous. Usually the heterogeneity within all the other steps (specified in Fig. 1) that occur between drug presence at the pharmacological receptor biophase and the measured effect is not appreciated in these theories. In cases where the subeffector units are not a homogeneous population, it affects the shape of the apparent concentration–effect relationship (i.e., the pharmacodynamics) as discussed below.

It is quite common to find that the binding process of ligands is not simple and that it frequently exhibits negative characteristics, e.g., an upwardly concave Scatchard plot (4,5). The question often arises as to whether such behavior results from genuine site–site interactions leading to negatively cooperative binding or whether the data reflect the binding of ligands to a heterogenous population of sites (5).

The sequence of reactions (between ligand binding and final response) essentially forms a "cascade amplifier" in which one step limits the maximal attainable effect. With gradual increase in the initial stimulus, one of the steps in the sequence will be the first to reach saturation, long before the initial stimulus reaches its maximal level (i.e., maximum receptor occupancy). Questions are raised, such as: Is the point of saturation in all the subeffector units in the population uniform? Is the sensitivity of each subeffector unit identical? New techniques like cloning of receptor cDNAs or genes have revealed heterogeneity far greater than had ever been anticipated from pharmacological analysis. Moreover, advanced procedures have enabled quantitative measurement of hormone release from individual cells, identification of channel subpopulations, and even monitoring the association between stimulant concentration and the response of a single channel in the cell membrane. In many cases (as detailed below), the results of investigations using such techniques support the concept of heterogeneity in the subeffector units.

The aim of this paper is to show the relationship between the subeffector unit heterogeneity and the value of the shape factor N. The subeffector units are defined here to contribute independently (of each other) to the pharmacological effect.

THEORETICAL

All-or-None Response Characteristic of the Subeffector Unit

Consider an all-or-none response with biological variation in the concentration at which the response is triggered. As recognized by Gaddum (8) and later by others (1,9), the biological variation determines the slope of the "population" (log) concentration–effect curve. This is because the observed concentration–effect relationship is actually the cumulative profile of the responses from each of the subeffector units, and according to Eq. (4) the sigmoidicity of this profile is defined by the shape factor N. Specifically, this means that N is directly related to the distribution function of the microparameters characterizing the population of subeffector units, including: (i) the threshold sensitivity of each unit, and (ii) the maximal response produced by each of the units. This relationship can be mathematically defined for the case of on–off behavior θ^* of the subeffector units as

$$\theta^*(C, EC_{50}) = \begin{cases} 1 & C > EC_{50}^* \\ 0 & C \leq EC_{50}^* \end{cases} \tag{5}$$

Here the concentration (C) – effect (E) relationship of the subeffector units is determined by the threshold concentration of each subeffector action (EC_{50}^*) and the corresponding maximal effect $E_{\max}^*$. This is illustrated for a single subeffector unit in Fig. 2.

If the distribution function of the threshold concentrations is defined as $\Psi(EC_{50}^*)$ then the observed concentration–effect relationship is described by

$$\frac{E_{\max} C^N}{EC_{50}^N + C^N} = \int_0^{\infty} \theta^*(C, EC_{50}) \Psi(EC_{50}^*)\, d(EC_{50}^*) = \int_0^C \Psi(\varepsilon)\, d\varepsilon \tag{6}$$

Where (the last part) is the integral of the function Ψ between 0 to C.

By using the fundamental theorem of calculus (10) we can differentiate Eq. (6) by C to yield

$$\Psi(x) = \frac{d}{dC}\left(\frac{E_{\max} C^N}{EC_{50}^N + C^N}\right)\Bigg|_{C=X} = E_{\max} N EC_{50}^N \frac{X^{N-1}}{(EC_{50}^N + X^N)^2} \tag{7}$$

This equation precisely determines the density function of EC_{50}^* that generates the observed concentration–effect relationship [i.e., Eq. (4)]. The pattern

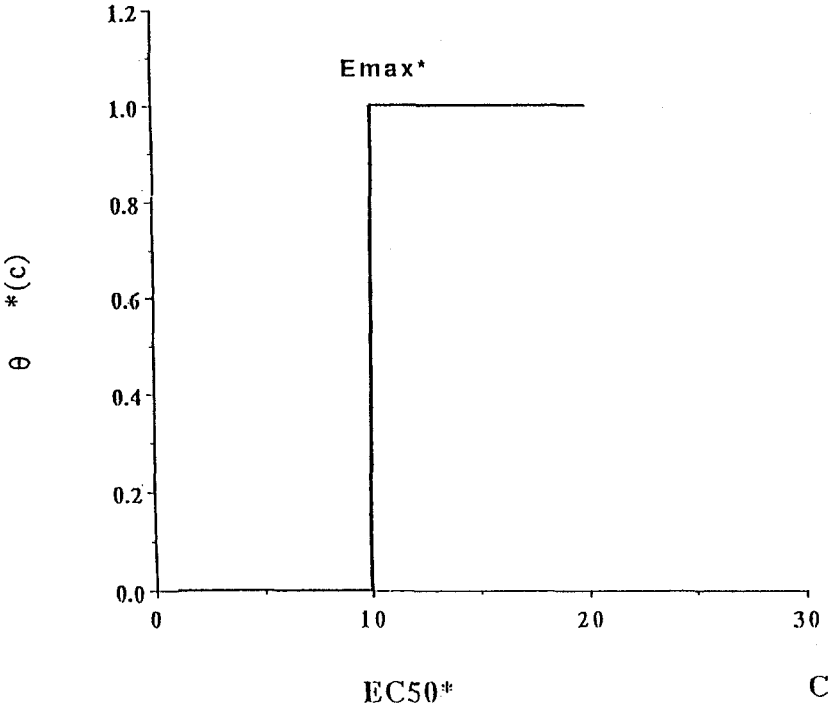

Fig. 2. The relationship between drug concentration and the magnitude of effect of a single effector unit in case of an all-or-none response.

of this density function is illustrated in Fig. 3 by numerical simulation of Eq. (7).

Ariens *et al.* (1) indicated that a certain distribution—namely, (log) Gaussian distribution of the threshold sensitivity—will ensure that the apparent pharmacodynamic profile will follow the E_{max} model [Eq. (3)], which is a special case of Eq. (4) with $N=1$.

There is a functional relationship between the value of N and the standard deviation (SD) of the subeffector unit distribution. The relationship depends on the EC_{50} value and can be described as

$$\frac{1}{1+(1/1+\alpha)^N}-\frac{1}{1+(1/1-\alpha)^N}=0.668 \tag{8}$$

Where $\alpha=\mathrm{SD}/EC_{50}$ (for a detailed mathematical derivation see Appendix A). It should be noted that SD is defined here as the symmetric interval around EC_{50} that includes 0.668 of all EC_{50}^* values.

The relationship between N and SD of the EC_{50}^* is illustrated in Fig. 4. For a given EC_{50} the greater the SD value, the lower the N. Hence in the

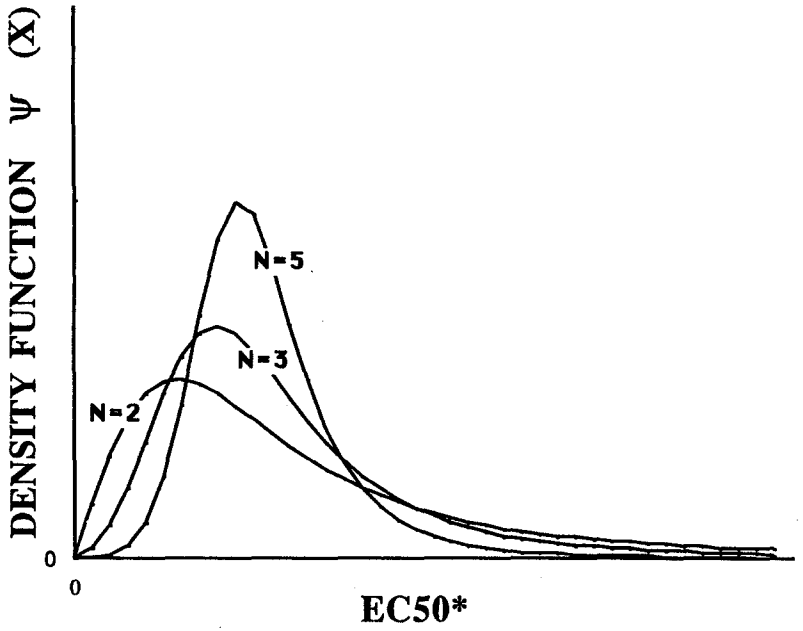

Fig. 3. Illustration of the relationship between the density function of EC_{50}^{*} and the apparent shape factor N.

case of all-or-none behavior of the individual subeffector units N is a function of the heterogeneity in the subeffector units.

The Pharmacodynamics of Subeffector Units: The General Case

The relationship between the available drug concentration seen by each subeffector unit and the intensity of response that it produces can be described as

$$E^{*} = E_{0}^{*} + \frac{E_{\max}^{*} C^{N^{*}}}{EC_{50}^{*N^{*}} + C^{N^{*}}} \tag{9}$$

The symbol * denotes that this is the value of the individual subeffector unit. Equation (9) is a general equation that can also be used to describe the case of all-or-none behavior of the subeffector unit, discussed above, i.e., the N^{*} value is large ($N > 5$).

Heterogeneity in the pharmacodynamics of the subeffector units can actually be derived from variability in the values of each of the parameters characterizing the pharmacodynamic profile of each of the subeffector units, i.e., E_{0}^{*}, $E_{\max}^{*}$, N^{*}, and EC_{50}^{*}. It is therefore of interest to understand how

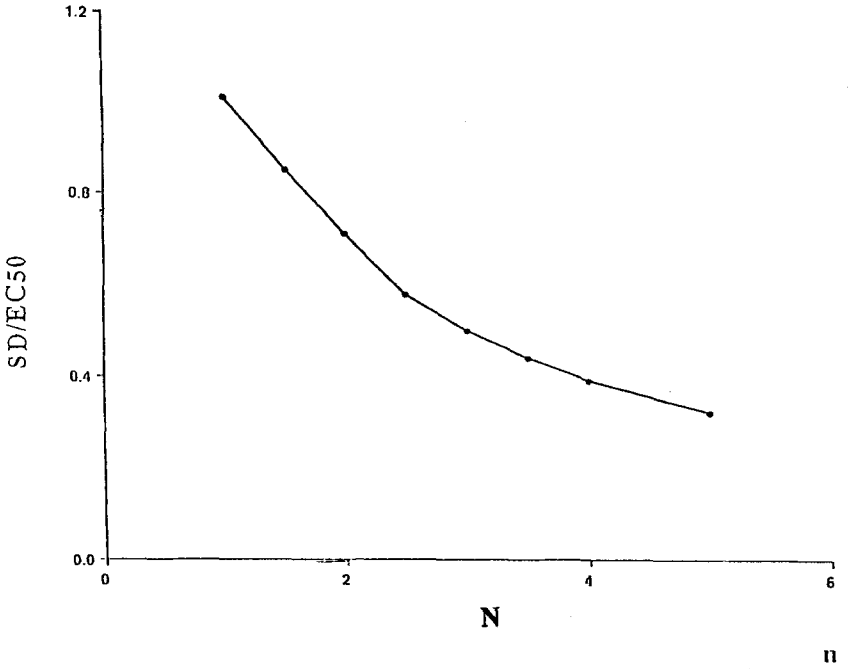

Fig. 4. Simulation of the relationship between N and SD of the EC_{50}^* according to Eq. (8).

variability in every one of these parameters could affect the value of N which determines the shape of the observed Effect–Concentration profile.

Equation (10) is the sigmoidal E_{max} equation in a basic form relating the apparent E and microparameters determining the value of effect for each subeffector unit (E^*) and the density function ϕ.

$$E(E_0, E_{max}, EC_{50}, N, C)$$

$$= \int E(E_0^*, E_{max}^*, EC_{50}^*, N^*, C)\phi(E_0^*, E_{max}^*, EC_{50}^*, N^*)$$

$$\times dE_0^*\, dE_{max}^*\, dEC_{50}^*\, dN^* \tag{10}$$

This equation can be written also as

$$E = \int E_0^* \phi\, dE_0^*\, dE_{max}^*\, dEC_{50}^*\, dN^* + \int dEC_{50}^*\, dN^*$$

$$\times \left(\frac{C^{N^*}}{EC_{50}^{*N^*} + C^{N^*}} \left[\int \phi(E_0^*, E_{max}^*, EC_{50}^*, N^*) E_{max}^*\, dE_{max}^*\, dE_0^* \right] \right) \tag{11}$$

The right term vanishes when $C=0$. The left term is a constant numerical value which is independent of C and therefore equals E_0. The term in the square brackets (which will be regarded as Z) is a function that depends solely on EC_{50}^* and N^*. Therefore, it can be concluded that the variability in E_{max}^* values among the subeffector units does not affect the shape factor N of the ensemble equation. This leads to Eq. (12) that shows more clearly that N is dependent only on function Z which in fact is the density function of N^* and EC_{50}^*.

$$E=E_0+\int [C^{N^*}/(EC_{50}^{*N^*}+C^{N^*})]Z(N^*, EC_{50}^*)\, dN^*\, dEC_{50}^* \qquad (12)$$

Furthermore, when C is taken to infinity, Eq. (12) is reduced to have the form of

$$E_{max}=\int Z(N^*, EC_{50}^*)\, dN^*\, dEC_{50}^* \qquad (13)$$

Equation (13) denotes that E_{max} depends upon Z.

To facilitate the mathematical derivations, the value of N^* will be regarded as a constant parameter. This also has biological connotations, and means that a certain value of N^* characterizes a specific pharmacological response.

The value of N can be calculated according to

$$N=\frac{4EC_{50}}{E_{max}}\frac{\partial E}{\partial C}\bigg|_{C=EC_{50}} \qquad (14)$$

This equation was obtained from the sigmoidal E_{max} equation. [Eq. (4)] (see Appendix B for the full derivation). This mathematical definition of N is actually wider than that denoted by Eq. (4) and includes all functions that have sigmoidal shape (on log concentration scale). This approach is required in order to analyze the changes in N value in different situations. For that, it is more convenient to replace the commonly used sigmoidal E_{max} equation [Eq. (4)], that is used to characterize the empirical concentration–effect data, with Eq. (15), which resembles very closely the pattern of Eq. (4).

$$E=E_0+E_{max}\, Erf[N\sqrt{\pi/8}(\lambda-\lambda_{50})], \qquad \lambda=\ln C, \quad \lambda_{50}=\ln EC_{50} \qquad (15)$$

Here λ equals $\ln(C)$, λ_{50} equals $\ln(EC_{50})$, and N follows Eq. (14). The term "Erf" is a commonly used function in statistics (11) that is employed to calculate the area under the normal (Gaussian) distribution curve and has

the following form:

$$Erf(X) = (1/\sqrt{2\pi}) \int_{-\infty}^{X} e^{-u^2/2}\, du \tag{16}$$

Rewriting Eq. (12) according to the concept of Eq. (15) provides

$$E = E_0 + \int Erf[N^*\sqrt{\pi/8}(\lambda - \lambda_{50}^*)]Z(\lambda_{50}^*)\, d\lambda_{50}^* \tag{17}$$

Following differentiation of Eq. (17) with respect to λ yields

$$\left(\frac{N}{4}\right) e^{-N^2\pi/16(\lambda-\lambda_{50})^2} = \left(\frac{N^*}{4}\right) \int e^{-N^{*2}\pi/16(\lambda-\lambda_{50}^*)^2} Z(\lambda_{50}^*)\, d\lambda_{50}^* \tag{18}$$

In the case where EC_{50}^* follows a log-normal distribution function Eq. (18) takes the form

$$NE_{\max}\, e^{-N^2\pi(\lambda-\lambda_{50})^2/16} = \int_{-\infty}^{\infty} e^{-N^{*2}\pi(\lambda-\lambda_{50}^*)^2/16} \times (A/\sqrt{2\pi\sigma})\, e^{-(\lambda_{50}^*-\lambda_{50})^2/2\sigma^2}\, d\lambda_{50}^* \tag{19}$$

where σ is the standard deviation of (the log form of) this function. Mathematical manipulations of Eq. (19) (specified in Appendix C) lead to the relationship between N, N^* and σ

$$N^2 = N^{*2} - \frac{N^{*4}\pi}{N^{*2}\pi + 8/\sigma^2} \tag{20}$$

From this relationship it is apparent that in case of heterogeneity of the subeffector units ($\sigma > 0$) the value of N is lower than N^*. Similarly, when σ equals 0 (i.e., in case of homogeneity) $N = N^*$. A very shallow apparent concentration–effect relationship will result in cases where σ tends to infinity. Further illustrations of the relationship between N and N^* at different σ values are presented in Fig. 5.

In practical cases, the values of N^* and σ are not available. Therefore, Fig. 6 shows what pairs of N^* and σ values produce an apparent N value.

When N^* is not a constant parameter, and is also different between the subeffector units, the system becomes more complex (mathematically) with a two dimensional distribution function. In the (special) case where EC_{50}^* is constant, the apparent N is an arithmetic average of N^* as evidenced from Eq. (14). In case where both EC_{50}^* and N^* vary the apparent N is a function of the distribution of both parameters.

A special case that takes place in practical situations is a descrete heterogeneity of the subeffector population. This means that the observed

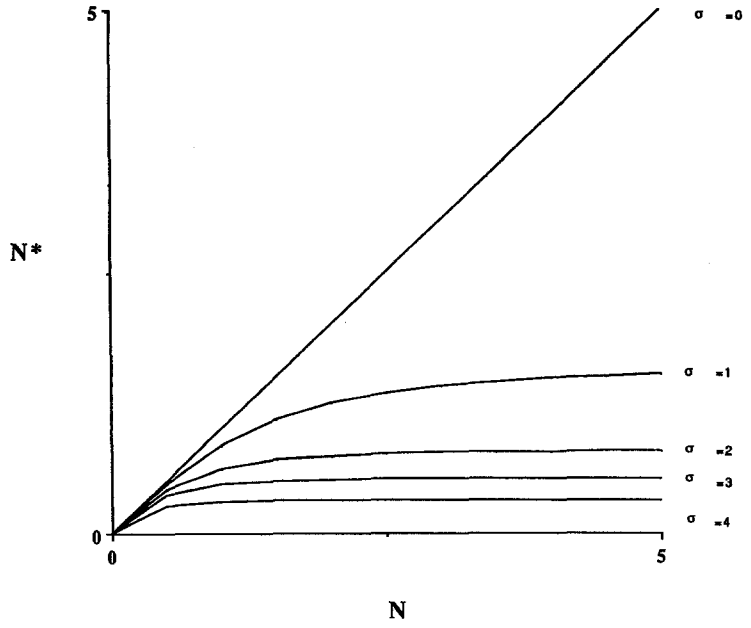

Fig. 5. The relationship between N^* and N at different σ values. σ is the SD of the log EC_{50}^*.

pharmacodynamic profile is an ensemble of a small (finite) number of different classes of concentration–effect relationships for the same drug or hormone. This case is similar in certain modes to the additive effect of two or more agonistic drugs (or endogenous stimulants) that is commonly encountered in pharmacodynamic investigations, and obviously to the cases in which the measured effect is related to more than one type of receptor, e.g., the effect of clonidine on pain (12). In that case the measured response is considered to be the sum of several sigmoidal E_{max} equations with the form of

$$E=\frac{E_{max}^1 C^{N1}}{EC_{50}^{N1}+C^{N1}}+\frac{E_{max}^2 C^{N2}}{EC_{50}^{N2}+C^{N2}} \tag{21}$$

This type of mathematical modeling is clearly required in cases where the concentration–effect relationship has a steplike shape. Such a pattern emerges when the (apparent) cumulative pharmacodynamic profile is the product of a certain number of populations with a clearly distinct EC_{50}^* value. However, if these EC_{50}^* values would not be so distinct, it would provide an apparent N that is smaller than N^*. In this case the apparent N value is the median (weighted mean) as shown in Fig. 7. The category of

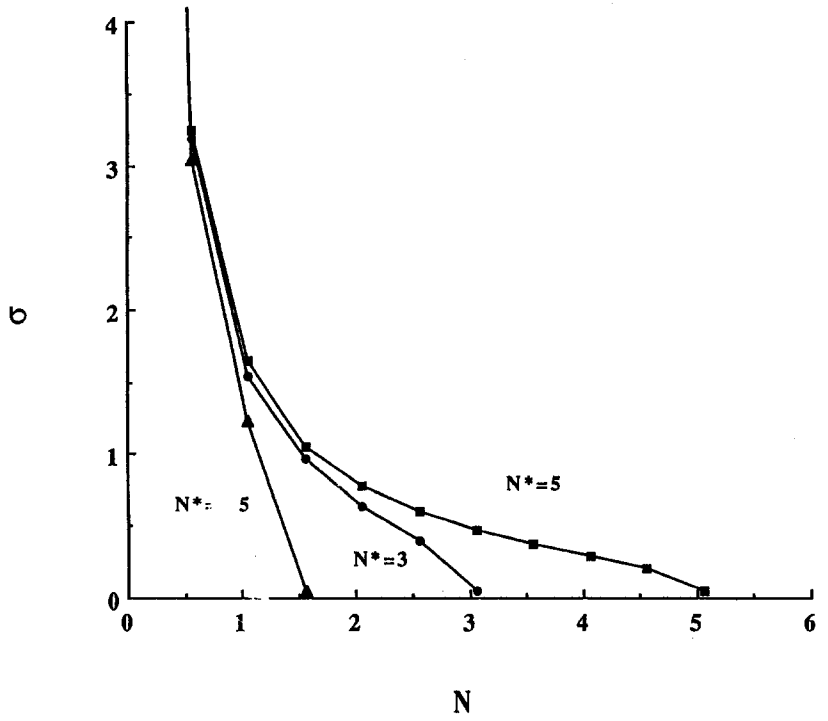

Fig. 6. Simulation according to Eq. (20) to demonstrate which pairs of N^* and σ values produce an apparent N value.

finite (discrete) heterogeneity is actually a unique condition of the general case of effector unit heterogeneity described above.

Another practical special case that is encountered during investigations is the situation where the concentration–effect relationship of each small entity (e.g., whole cell) follows the sigmoid E_{max} model [Eq. (4)] while the single subeffector unit of which the "small entity" is composed (e.g., specific ion channels) exhibits quantal (all-or-none) behavior. The heterogeneity of each of these parameters (i.e., the subeffector units and the small entity) follow different density functions. The overall pattern will be influenced by the two distribution functions. Practically, this situation can be treated as an undivided case, depending upon the available information. It can be dealt with either according to the data of the quantal behavior exhibited by the single subeffector unit or by considering the data of the small entity as composed of many single subeffector units that follow the shape of Eq. (9) (e.g., whole cells data).

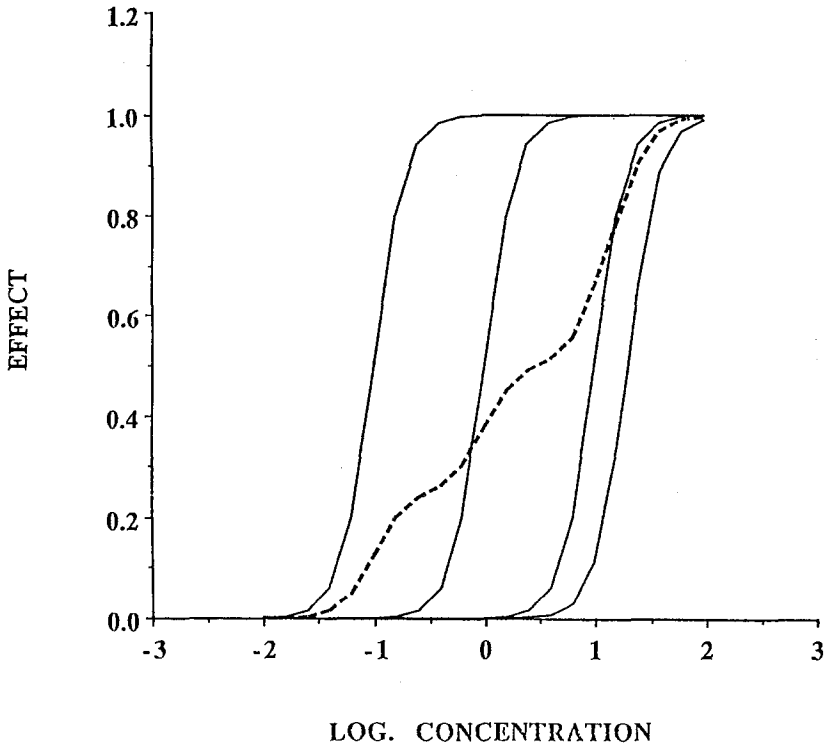

Fig. 7. The shape of the apparent concentration–effect profile (broken line) in case of discrete heterogeneity. The magnitude of the effect of each profile is normalized to give maximal $E=1$.

DISCUSSION

Indications for Heterogeneity in Subeffector Units

The issue of receptor heterogeneity has been investigated for many years and is still in the forefront of life science research (13). Until now most of the attention has focused on heterogeneity in ligand–receptor binding properties (5,6,13), rather than at the concentration–effect level. For instance, the finding that intrinsic activity (the ability of an agonist to cause an effect) can vary independently of chemical binding has been disregarded (14). Current investigational methods have revealed that not only do receptors have an astonishing variety of subtypes but also the components of the "amplifying system" such as the G-proteins, are composed of several subunits, each of which has a great degree of variability (15). The different subtypes give rise to a variety of different oligomeric isoforms with different

pharmacological sensitivities. In addition, as can be seen by the variety of examples delineated below, heterogeneity in subeffectors units is quite common in biological systems and is part of the regulatory processes of the stimulus–response system in normal physiology. Most of the examples have been taken from physiological responses that are normally activated by endogenous regulatory ligands (e.g., hormones, neurotransmitters), since many drugs act on such physiological receptors.

The examples for heterogeneity in subeffector unit populations cover data from various types of biological processes including (i) hormone secretion; (ii) response to a hormonal stimulus; (iii) activity of second messengers; (iv) stimulus-evoked synaptic currents; and (v) ion channels.

Hormone Secretion. Unlike the traditional method of evaluating secretory activity by measuring hormone release in cell supernatants, recent investigations examining endocrine secretion from individual cells have provided convincing evidence for heterogeneity in the response of cells. These results oppose the classical stimulus–secretion coupling theory that suggests that each cell responds to a given stimulus with the release of secretory product. The evidence found so far includes parathyroid hormone (PTH) cells (16); pancreatic beta-cells (17,18); the gonadotropes—luteinizing hormone releasing cells (19); pituitary cells (20); and porcine somatotrophs (21).

Response to a Hormonal Stimulus. Evidence of variability in cellular responsiveness to hormone stimulus includes antidiuretic hormone (ADH) which reflect inherent heterogeneity of granular cell reactivity to the hormone (22); actin polymerization in human blood platelets (23); considerable cell to cell variations in cytosolic Ca^{2+} in response to epidermal growth factor stimulus (24,25); evidence that hormone-evoked calcium release from intracellular stores is a quantal rather than a continuous process (26).

Activity of Second Mesenger. Current studies (26–28) provide direct evidence that Inositol 1,4,5 triphosphate ($InsP_3$)-induced Ca^{2+} liberation is quantized and have suggested that the $InsP_3$-sensitive Ca^{2+} pool may be a collection of independent, localized compartments that release Ca^{2+} in an all-or-none manner.

Stimulus-Evoked Synaptic Currents. The variability in miniature excitatory postsynaptic current amplitude arises predominantly from variability within a single bouton (29–32).

Ion Channels. Because of advanced research techniques we are now able to see electrophysiological heterogeneity in single-channels. For instance, using a patch-clamp study in a pituitary slice preparation, it was shown that GABA-mediated synaptic transmission in neuroendocrine cells has an all-or-nothing character of stimulus evoked synaptic currents (34). Na^+ channel expression in lactopore subpopulations of rat is not uniform

(35). Electrophysiological analysis following specific activation of a human K^+ channel gene has also disclosed heterogeneity in the currents recorded from single channels at a constant stimulus (+30 mV) (36).

In addition, the overall thesis of heterogeneity in drug concentration–effect relationship at the subeffector level is also supported by the known heterogeneity in blood cells (23,37), mast cells (38), and hepatocytes (39).

In many cases a heterogeneous subeffector unit population is composed of a discrete distribution of receptor subtypes. A phenomenon of receptor subtypes that show considerable variation not only in the binding affinity but also in the sensitivity to the same adrenergic molecule (e.g., norepinephrine) has been demonstrated in arteries taken from different sites in the body (14). In certain cases, heterogeneity of receptor and postreceptor apparatus in different parts of the same organ may be related to basic concepts of topoendocrinology (40).

There are many cases in which the sigmoidal E_{max} model was employed to assess a pharmacodynamic profile constructed by the number of individuals (patients) who required a certain threshold concentration of the drug to produce a defined pharmacologic response (41,42). This is a case of an all-or-none response that is analogous to that of quantal response in heterogeneous subeffector unit population that was described above. The apparent N value in this case is also a function of the distribution density function of the individual threshold of drug concentration. Analogous discrepancies between individual subunits and the apparent profile representing an ensemble of these subunits was also described before in another pharmaceutical discipline—*in vitro* release kinetics from microparticulate systems (43,44).

Pharmacodynamic Implications of Effector Unit Heterogeneity

As demonstrated above, heterogeneity of subeffector units and/or cell subpopulations normally exist in physiology and consequently in pharmacology. This phenomenon is reflected in the relationship between the stimulant concentration and the intensity of the response it induces. This idea was suggested long ago (1) but was not substantiated. Currently available research techniques enable us to monitor activity patterns of single cells and even single channels. Thus, we can now demonstrate that in various cases in which a stimulant concentration–effect relationship at the level of a single cell follows a continuous function [e.g., Eq. (9)], it may be actually derived from quantal behavior of the individual channels. In case of heterogeneity of the (sub)effector units the apparent concentration–effect relationship which is the overall pattern of the ensemble of units does not reveal the pattern of the single subunit. This is the reason why the role of subeffector

unit heterogeneity in influencing the shape of the concentration–effect relationship has not been clearly appreciated until now. As has been demonstrated here the heterogeneity in E_0^* and E_{max}^* values do not affect the shape of the concentration effect profile, whereas variability in EC_{50}^* and N^* are crucial in determining N value. The mathematical principles which relate the concentration–effect profile of the individual subeffector unit [Eq. (9)] and the apparent pharmacodynamic profile [Eq. (4)] are fundamental for concentration–effect investigations. It should be noted, however, that when the pharmacodynamic investigations are performed in an intact animal there could be certain deviations between the measured effect of the drug and the initial stimulus due to the fact that the empirical description of the relationship between plasma or effect site concentration and the observed effect is not a clear reflection of the drug–effector unit interaction. Furthermore, it may be hard to distinguish *in vivo* independent effector units. Nevertheless, the principles associating subeffector unit heterogeneity and the shape of the pharmacodynamic profile of an observed pharmacologic response (as determined by N) should not be substantially different from pure pharmacologic investigations performed in cell cultures or similar isolated conditions. This is, of course, provided that the concentration–effect relationship under investigation is free of pharmacokinetic complexities (45).

APPENDIX A

The Relationship Among σ, N, and the EC_{50}

$$\int_{EC_{50}-\sigma}^{EC_{50}+\sigma} \Psi(x)\,dx = 0.668E_{max}$$

$$\left.\frac{E_{max}C^N}{EC_{50}^N + C^N}\right|_{EC_{50}-\sigma}^{EC_{50}+\sigma} = 0.668E_{max}$$

$$\frac{(EC_{50}+\sigma)^N}{(EC_{50}+\sigma)^N + EC_{50}^N} - \frac{(EC_{50}-\sigma)^N}{(EC_{50}-\sigma)^N + EC_{50}^N} = 0.668$$

$$\frac{1}{1+(1/(1+\sigma/EC_{50}))^N} - \frac{1}{1+(1/(1+\sigma/EC_{50}))^N}$$

where $x = \sigma/EC_{50}$

$$\frac{1}{1+(1/1+x)^N} - \frac{1}{1+(1/1-x)^N} = 0.668$$

APPENDIX B

The Derivation of N from the Concentration–Effect Relationship

$$\frac{\partial E}{\partial C}=\frac{\partial}{\partial C}\left(\frac{E_{\max}C^N}{EC_{50}^N+C^N}\right)=E_{\max}\frac{EC_{50}^N}{(EC_{50}^N+C^N)^2}NC^{N-1}$$

$$\left.\frac{\partial E}{\partial C}\right|_{C=EC_{50}}\frac{E_{\max}EC_{50}^N NEC_{50}^{N-1}}{(2EC_{50}^N)^2}=\frac{E_{\max}N}{4EC_{50}}$$

$$N=\frac{4EC_{50}}{E_{\max}}\left.\frac{\partial E}{\partial C}\right|_{C=EC_{50}}$$

APPENDIX C

The Mathmetical Derivation Leading from Equation (19) to Equation (20)

Let L be the left side and R the right side of Eq. (19).

$$\underset{\mathrm{L}}{NE_{\max}e^{-N^2\pi(\lambda-\lambda_{50})^2/16}}$$

$$=\int_{-\infty}^{\infty}\underset{\mathrm{R}}{e^{-N^{*2}\pi(\lambda-\lambda_{50}^*)^2/16}-(A/\sqrt{2\pi\sigma})\,e^{-(\lambda_{50}^*-\lambda_{50})^2/2\sigma^2}}\,d\lambda_{50}^* \quad (19)$$

Calculating the exponent term of R

$$N^{*2}\frac{\pi}{16}(\lambda-\lambda_{50}^*)^2+(\lambda-\lambda_{50}^*)^2/2\sigma^2$$

$$=\lambda_{50}^{*2}\left(\frac{1}{2\sigma^2}\right)+\lambda_{50}^*\left(\frac{\lambda_{50}}{\sigma^2}\right)+\left(\frac{\lambda_{50}^2}{2\sigma^2}+\frac{\lambda_{50}^2N^{*2}\pi}{16}-\frac{\lambda\lambda_{50}N^{*2}\pi}{8}-\frac{\lambda^2N^{*2}\pi}{16}\right)$$

By completing the square

$$A(\lambda_{50}^*-B)+C\lambda^2+D\lambda+E$$

For some constants A, B, C, D, E, which depend only on N^*, λ, and σ it is enough to calculate C.

$$R=K\,e^{-(C\lambda^2+D\lambda)}\text{ for some constant }K.$$

The calculations of C yield

$$C=\frac{\pi}{16}\left(n^{*2}-\frac{N^{*4}\pi}{N^{*2}\pi+8/\sigma^2}\right)$$

By comparing with the exponent of L it becomes

$$\frac{N^2\pi}{16} = C \Rightarrow N^2 = N^{*2} - \frac{N^{*4}\pi}{N^{*2}\pi + 8/\sigma^2}$$

which is Eq. (20).

REFERENCES

1. E. J. Ariens, A. M. Simonis, and J. M. van Rossum. The relation between stimulus and effect. In E. J. Ariens (ed.), *Molecular Pharmacology: The Mode of Action of Biologically Active Compounds*, Vol. 1, Academic Press, New York, 1964, pp. 394–466.
2. J. M. van Rossum and J. P. T. Burgers. Quantitative relationships between dynamics and kinetics of drugs: A system dynamics approach. *Drug Metab. Rev.* **15**:365–382 (1984).
3. A. V. Hill. The possible effects of the aggregation of the molecules of haemoglobin on the dissociation curves. *J. Physiol.* **40**:iv–vii (1910).
4. J. C. Kermode. The curvilinear scatchard plot: Experimental artifact or receptor heterogeneity?: *Biochem. Pharmacol.* **38**:2053–2060 (1989).
5. A. Levitzki (ed.). *Receptors: A Quantitative Approach*, Benjamin/Cummings Publishing, Menlo Park, CA, 1984.
6. A. Levitzki (ed.). *Quantitative Aspects of Allosteric Mechanisms*, Springer-Verlag, Berlin, 1978.
7. J. G. Wagner. Kinetics of pharmacologic response I. Proposed relationship between response and concentration in the intact animal and man. *J. Theoret. Biol.* **20**:173–201 (1968).
8. J. H. Gaddum. The quantitative effects of antagonistic drugs. *J. Physiol.* **89**:7P (1937).
9. E. J. Ariens, A. J. Beld, J. F. Rodrigues de Miranda, and A. M. Simonis. In R. D. O'Brien (ed.), *The Receptors: A Comprehensive Treatise*, Plenum Press, New York, 1979, pp. 33–92.
10. H. Courant. *Calculus*, 1984, p. 254.
11. R. C. Weast and S. M. Selby. In *Handbook of Mathematical Tables*, 2nd ed., Chemical Rubber Company, 1964, p. 272.
12. L. K. Paalzow. Integrated pharmacokinetic-dynamic modelling of drugs acting on the CNS. *Drug Metab. Rev.* **15**:383–400 (1984).
13. D. R. Burt and G. L. Kamatchi. GABAa receptor subtypes: from pharmacology to molecular biology. *FASEB J.* **5**:2916–2923 (1991).
14. J. A. Bevan, R. D. Bevan, and S. M. Shreeve. Variable receptor affinity hypothesis. *FASEB J.* **3**:1696–1704 (1989).
15. F. Boege, E. Neumann, and E. J. M. Helmreich. Structural heterogeneity of membrane receptors and GTP-binding proteins and its functional consequences for signal transduction. *Eur. J. Biochem.* **199**:1–15 (1991).
16. L. A. Fitzpatrick. Heterogeneous secretory response of parathyroid cells. *Recent Prog. Horm. Res.* **48**:471–475 (1993).
17. D. G. Pipeleers. Heterogeneity in pancreatic beta-cell population. *Diabetes* **41**:777–781 (1992).
18. D. Bosco, M. Chanson, R. Bruzzone, and P. Meda. Visualization of amylase secretion from individual pancreatic acini. *Am. J. Physiol.* **254**:G664–G670 (1988).
19. D. A. Leong and M. O. Thorner. A potential code of luteinizing hormone-releasing hormone-induced calcium responses in the regulation of luteinizing hormone secretion among individual gonadotrophs. *J. Biol. Chem.* **266**:9016–9020 (1991).
20. M. E. Kendall and W. C. Hymer. Cell blotting: a new approach to quantify hormone secretion from individual rat pituitary cells. *Endocrinology* **121**:2260–2262 (1987).

21. P. M. Dobado-Berrios, A. Ruiz-Navarro, R. Torronteras, and F. Gracia-Navarro. Application of an optimized immunostaining technique to evaluate the heterogeneous secretory response from porcine somatotrophs by cell blotting. *J. Histochem. Cytochem.* **40**:1715–1724 (1992).
22. W. A. Kachadorian, J. Muller, and V. A. DiScala. Variability of cellular responsiveness to ADH stimulation in toad urinary bladder. *Am. J. Physiol.* **256**:F590–F595 (1989).
23. A. Oda, J. F. Daley, C. Cabral, J. Kang, M. Smith, and E. W. Salzman. Heterogeneity in filamentous actin content among individual human blood platelets. *Blood* **79**:920–927 (1992).
24. F. A. Gonzalez, D. J. Gross, L. A. Heppel, and W. W. Webb. Studies on the increase in cytosolic free calcium induced by epidermal growth factor, serum, and nucleotides in individual A431 cells. *J. Cell Physiol.* **135**:269–276 (1988).
25. P. H. G. M. Willems, S. E. Van Emst-De Vries, C. H. Van Os, and J. J. H. H. M. De Pont. Dose-dependent recruitment of pancreatic acinar cells during receptor-mediated calcium mobilization. *Cell Calcium* **14**:145–159 (1993).
26. S. Muallem, S. J. Pandol, and T. G. Beeker. Hormone-evoked calcium release from intracellular stores is a quantal process. *J. Biol. Chem.* **264**:205–212 (1989).
27. L. Parker and I. Ivorra. Localized all-or-none calcium liberation by inositol triphosphate. *Science* **250**:977–979 (1990).
28. K. A. Oldershaw, D. L. Nunn, and C. W. Taylor. Quantal Ca2+ mobilization stimulated by inositol 1,4,5-triphosphate in permeabilized hepatocytes. *Biochem. J.* **278**:705–708 (1991).
29. J. M. Bekkers, G. B. Richerson, and C. F. Stevens. Origin of variability in the quantal size in cultured hippocampal neurons and hippocampal slices. *Proc. Natl. Acad. Sci. U.S.* **87**:5359 (1990).
30. K. P. Scholz and R. J. Millet. Inhibition of quantal transmitter release in the absence of calcium influx by a G protein-like adenosine receptor at hippocampal synapses. *Neuron* **8**:1139–1150 (1992).
31. A. Malgaroli and R. W. Tsien. Glutamate-induced long-term potentiation of the frequency of miniature synaptic currents in cultured hippocampal neurons. *Nature* **357**:134–139 (1992).
32. C. R. Lupica, W. R. Proctor, and T. V. Dunwiddie. Presystemic inhibition of excitatory synaptic transmission by adenosine in rat hippocampus: Analysis of unitary EPSP variance measured by whole-cell recording. *J. Neurosci.* **12**:3753–3764 (1992).
33. C. Newland, D. Colquhoun, and S. G. Cull-Candy. Single channels activated by high concentrations of GABA in superior cervical ganglion neurons of the rat. *J. Physiol.* **432**:203–233 (1991).
34. R. Scheneggenburger and A. Konnerth. GABA-mediated synaptic transmission in neuroendocrine cells: a patch-clamp study in a pituitary slice preparation. *Pfluegers Arch.* **421**:364–373 (1992).
35. J. Horta, M. Hiriart, and G. Cota. Differential expression of Na channels in functional subpopulations of rat lactopores. *Am. J. Physiol.* **261**:C865–C871 (1991).
36. P. A. Shelton, N. W. Davies, M. Antoniou, F. Grosveld, M. Needham, M. Hollis, W. J. Brammar, and E. C. Conley. Regulated expression of K^+ channel genes in electrically silent mammalian cells by linkage to beta-globin gene-activation elements. *Recept. Channel* **1**:25–37 (1993).
37. M. K. Taylor and J. J. Cohen. Cell-mediated cytotoxicity. *Curr. Opin. Immunol.* **4**:338–343 (1992).
38. M. A. Lowman, P. H. Rees, R. C. Benyon, and M. K. Church. Human mast cell heterogeneity: Histamine release from mast cells dispersed from, skin, lung, adenoids, tonsils, and colon in response to IgE-dependent and nonimmunologic stimuli. *J. Allergy Clin. Immunol.* **81**:590–797 (1988).
39. R. A. Wilson and J. R. Hart. In vivo drug metabolism and liver lobule heterogeneity in the rat. *Gastroenterology* **81**:563–569 (1981).
40. L. M. Berstein. Topoendocrinology. *J. Endocrinol.* **137**:163-166 (1993).

41. M. E. Ausems, C. C. Hug, D. R. Stanski, and A. G. L. Plasma concentrations of alfentanil required to supplement nitrous oxide anesthesia for general surgery. *Anesthesiology* **65**:362–373 (1986).
42. A. S. Nies. Principles of therapeutics. In A. Goodman Gilman, L. S. Goodman, T. W. Rall, and F. Murad (eds.), *Goodman and Gilman's The Pharmacological Basis of Therapeutics*, 7th ed., MacMillan, New York, 1985, pp. 62–83.
43. S. T. Gross, A. Hoffman, M. Donbrow, and S. Benita. Fundamentals of the release mechanism interpretation in multiparticulate systems: the prediction of the commonly observed release equations from statistical population models for particle ensembles. *Int. J. Pharm.* **29**:213–222 (1986).
44. A. Hoffman, M. Donbrow, S. T. Gross, S. Benita, and R. Bahat. Fundamentals of release mechanism interpretation in multiparticulate systems: Determination of substrate release from single microcapsules and relation between individual and ensemble release kinetics. *Int. J. Pharm.* **29**:195–211 (1986).
45. M. Danhof, J. W. Mandema, and A. M. Stijnen, In C. J. van Boxtel, N. H. G. Holford, and M. Danhof (eds.), *The In Vivo Study of Drug Action*, Elsevier, Amsterdam, 1992, pp. 29–58.